

Article

Selenium Minerals: Structural and Chemical Diversity and Complexity

Vladimir G. Krivovichev ^{1,*}, Sergey V. Krivovichev ^{1,2} and Marina V. Charykova ¹¹ Institute of Earth Sciences, St. Petersburg State University, University Emb. 7/9, 199034 St. Petersburg, Russia² Nanomaterials Research Centre, Kola Science Centre, Russian Academy of Sciences, Fersmana 14, 184209 Apatity, Russia

* Correspondence: vkrivovi@yandex.ru

Received: 27 June 2019; Accepted: 21 July 2019; Published: 23 July 2019



Abstract: Chemical diversity of minerals containing selenium as an essential element has been analyzed in terms of the concept of mineral systems and the information-based structural and chemical complexity parameters. The study employs data for 123 Se mineral species approved by the International Mineralogical Association as of 25 May 2019. All known selenium minerals belong to seven mineral systems with the number of essential components ranging from one to seven. According to their chemical features, the minerals are subdivided into five groups: Native selenium, oxides, selenides, selenites, and selenates. Statistical analysis shows that there are strong and positive correlations between the chemical and structural complexities (measured as amounts of Shannon information per atom and per formula or unit cell) and the number of different chemical elements in a mineral. Analysis of relations between chemical and structural complexities provides strong evidence that there is an overall trend of increasing structural complexity with the increasing chemical complexity. The average structural complexity for Se minerals is equal to 2.4(1) bits per atom and 101(17) bits per unit cell. The chemical and structural complexities of O-free and O-bearing Se minerals are drastically different with the first group being simpler and the second group more complex. The O-free Se minerals (selenides and native Se) are primary minerals; their formation requires reducing conditions and is due to hydrothermal activity. The O-bearing Se minerals (oxides and oxysalts) form in near-surface environment, including oxidation zones of mineral deposits, evaporites and volcanic fumaroles. From the structural viewpoint, the five most complex Se minerals are marthozite, $\text{Cu}(\text{UO}_2)_3(\text{SeO}_3)_2\text{O}_2 \cdot 8\text{H}_2\text{O}$ (744.5 bits/cell); mandarinoite, $\text{Fe}_2(\text{SeO}_3)_3 \cdot 6\text{H}_2\text{O}$ (640.000 bits/cell); carlosruizite, $\text{K}_6\text{Na}_4\text{Na}_6\text{Mg}_{10}(\text{SeO}_4)_{12}(\text{IO}_3)_{12} \cdot 12\text{H}_2\text{O}$ (629.273 bits/cell); prewittite, $\text{KPb}_{1.5}\text{ZnCu}_6\text{O}_2(\text{SeO}_3)_2\text{Cl}_{10}$ (498.1 bits/cell); and nicksobolevite, $\text{Cu}_7(\text{SeO}_3)_2\text{O}_2\text{Cl}_6$ (420.168 bits/cell). The mechanisms responsible for the high structural complexity of these minerals are high hydration states (marthozite and mandarinoite), high topological complexity (marthozite, mandarinoite, carlosruizite, nicksobolevite), high chemical complexity (prewittite and carlosruizite), and the presence of relatively large clusters of atoms (carlosruizite and nicksobolevite). In most cases, selenium itself does not play the crucial role in determining structural complexity (there are structural analogues or close species of marthozite, mandarinoite, and carlosruizite that do not contain Se), except for selenite chlorides, where stability of crystal structures is adjusted by the existence of attractive Se–Cl closed-shell interactions impossible for sulfates or phosphates. Most structurally complex Se minerals originate either from relatively low-temperature hydrothermal environments (as marthozite, mandarinoite, and carlosruizite) or from mild (500–700 °C) anhydrous gaseous environments of volcanic fumaroles (prewittite, nicksobolevite).

Keywords: selenium minerals; mineral systems; structural complexity; chemical complexity; Shannon information

1. Introduction

Mineral ecology is a direction in mineralogical research that considers factors that influence mineral distribution, diversity, and complexity through space and time [1–3]. The concept of mineral ecology is relatively recent [1], though many ideas that lie behind the basic principles of this approach have been formulated and discussed in Russian mineralogical literature since Vladimir Vernadsky's "History of the Minerals of the Earth's Crust" [4]. The contributions by Fersman [5], Saukov [6], Povarennykh [7], Urusov [8,9], Ivanov and Yushko-Zakharova [10], Khomyakov [11], Yaroshevsky [12], and others should be particularly mentioned. The advent of new digital technologies of big-data analysis revolutionized the field, leading to many important insights into chemical, structural and genetic relations between different groups of minerals and formulation of a new research direction of data-driven discovery in Mineralogy [13–16].

Yushkin [17] pointed out the necessity of formulation of quantitative criteria that would describe the state of the mineral kingdom at certain stages of its time development, and Petrov [18], Bulkin [19,20], and Yushkin [21] indicated that Shannon informational (entropy) approach can be employed to measure chemical complexity and diversity of geochemical and mineralogical systems. S. Krivovichev [22–26] proposed to use Shannon information content for the quantitative analysis of structural complexity of minerals and inorganic compounds and outlined basic applications of this approach to the understanding of structural evolution of minerals and mineral associations. It was also demonstrated that structural complexity parameters are directly related to configurational entropy of crystalline solids [27]. An alternative approach was proposed by V. Krivovichev and Charykova [28,29] and Grew et al. [30] on the basis of the concept of mineral systems, which provides a useful tool for the chemical classification of mineral species and allows to arrange the existing data into coherent frameworks emphasizing changes in mineral diversity and composition with time. Using the concept of mineral systems, different geological objects were compared from the viewpoint of their mineral diversity as exemplified by highly alkaline massifs (Khibiny, Lovozero, Russia, and Mont Saint-Hilaire, Canada) [31], evaporite deposits (Inder, Kazakhstan, and Searles Lake, USA) [32], fumaroles at active volcanoes (Tolbachik, Kamchatka, Russia, and Vulcano, Sicily, Italy) [33], and famous hydrothermal deposits such as Otto Mountain, USA, and El Dragon, Bolivia [34].

The concepts of mineral systems and complexities (chemical and structural) have also been applied to the mineral evolution as a whole. Following [35,36], four groups of minerals were considered corresponding to the four eras of mineral evolution: "Ur-minerals", minerals from chondritic meteorites, Hadean minerals, and minerals of the modern era. These four different stages were compared in terms of their mineral diversity (the number of mineral species) and the chemical and structural complexities. The quantitative analysis of mean chemical and structural complexities for the four groups demonstrate, with reasonably strong discriminative power, that both chemical and structural complexities are gradually increasing in the course of mineral evolution [37,38].

This study is focused on the mineral ecology of Se minerals. The chemistry of selenium resembles that of sulfur, owing to the proximity of the two elements in the periodic table. Similarly to sulfur, selenium adopts four different oxidation states: -2 (selenides), 0 (elemental selenium), $+4$ (selenites), and $+6$ (selenates). Se minerals are relatively rare, with only 123 mineral species presently known according to the International Mineralogical Association [39] (Supplementary Table S1). The majority of known Se minerals (87) are selenides. In O-bearing species, Se occurs as Se^{4+} and/or Se^{6+} cations. The latter has a lone pair of electrons and usually possesses an asymmetric trigonal pyramidal coordination, forming selenite (SeO_3)²⁻ anions with Se atom at the apical vertex of the pyramid. In contrast, Se^{6+} cations invariably form (SeO_4)²⁻ tetrahedra. However, natural selenates are unstable under oxidizing conditions and transform into selenites, which explains the rarity of selenates in nature.

Previously, we have characterized Se oxyalts (selenites and selenates) and evaluated the accuracies of thermodynamic constants of selenides and selenites [40,41]. The aim of this paper is to characterize Se minerals as natural mineral systems and to investigate relations between their chemical and

structural complexities, measured as Shannon information amounts, and to apply these measures to the understanding of Se minerals diversity and complexity.

2. Materials and Methods

2.1. Mineral Systems

As it has been mentioned above, there are only 123 Se mineral species known to date (Supplementary Table S1). It had been shown previously [28,29] that any mineral can be assigned to a specific chemical system, according to all elements that play species-defining roles in its chemical composition. The elements are chosen in agreement with the current rules of the new mineral species definition [42–44], taking into account the discussion of these problems in Russian literature. The chemical formulas of Se minerals used for the calculations are those approved by the International Mineralogical Association (IMA) and taken from the continuously updated lists published by Marco Pasero [39] at the website of the Commission on New Minerals, Nomenclature and Classification IMA (CNMNC IMA). Only species-defining chemical elements were taken into account, without consideration of isomorphic substitutions. The chemical system is identified in accord with the *thermochemical* sequence of chemical elements (Figure 1) [28]. For example, giraudite, $\text{Cu}_6\text{Cu}_4\text{Zn}_2(\text{AsSe}_3)_4\text{S}$, belongs to the system SSeAsZnCu , while prewittite, $\text{K}_2\text{Pb}_3\text{Zn}_2\text{Cu}_{12}(\text{SeO}_3)_4\text{O}_4\text{Cl}_{20}$, belongs to the system OCiSePbZnCuK .

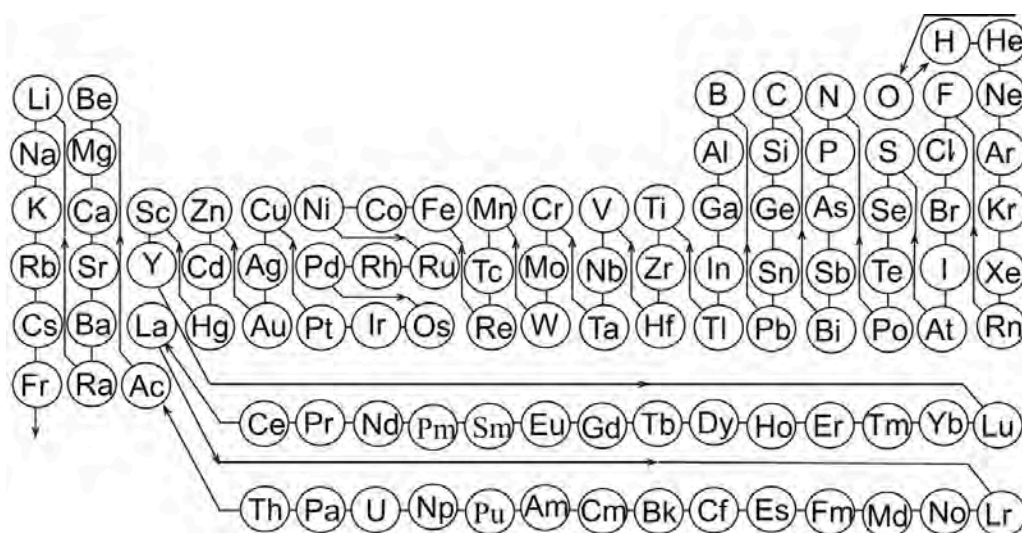


Figure 1. Thermochemical sequence of chemical elements and corresponding single-component systems. The arrows indicate the order used for the identification of a mineral system.

2.2. Chemical and Structural Complexity

For the investigation of structural and chemical complexity of minerals, a total of 123 datasets on the chemical compositions and 76 datasets on the crystal structures of Se minerals were considered. The amounts of structural Shannon information per atom ($^{str}I_G$) and per unit cell ($^{str}I_{G,total}$) were calculated using the approach developed by S. Krivovichev [22–25] according to the following equations:

$$^{str}I_G = - \sum_{i=1}^k p_i \log_2 p_i \quad (\text{bits/atom}) \quad (1)$$

$$^{str}I_G = -v \sum_{i=1}^k p_i \log_2 p_i \quad (\text{bits/cell}) \quad (2)$$

where k is the number of different crystallographic orbits (independent crystallographic Wyckoff sites) in the structure, and p_i is the random choice probability for an atom from the i th crystallographic orbit, that is:

$$p_i = m_i/v \quad (3)$$

where m_i is a multiplicity of a crystallographic orbit (i.e. the number of atoms of a specific Wyckoff site in the reduced unit cell), and v is the total number of atoms in the reduced unit cell.

For several hydrated crystal structures of Se minerals, the positions of H atoms have not been determined in the original structure reports. In these cases, the H-correction procedure was applied by introducing into structure model of surrogate H atoms [45].

The calculation of different contributions to structural complexity was done using the approach described by S. Krivovichev [26] and recently applied by Gurzhiy and Plasil [46] to the analysis of complexity of uranyl sulfates. The following contributions to the total structural complexity can be recognized: (1) topological complexity expressed as topological information (**TI**) corresponds to the complexity of a structural unit (or cluster) with a maximal degree of symmetry (for clusters, the cluster information (**CI**) is used (see below for details)), (2) structural complexity of a unit expressed as structural information (**SI**) corresponds to the complexity of a structural unit with real symmetry, (3) additional information arises from the layer stacking (**LS**) for the layered structures with multiple layers per unit cell, (4) complexity of the interstitial structure (**IS**) that occupies the space between (or within for framework structures) structural units, (5) complexity due to the hydrogen bonding (**HB**) system calculated as a contribution of hydrogen atoms towards total complexity [26]. The method allows one to estimate contributions of different factors to the total structural complexity in quantitative terms, either in bits/cell or in percent (see below). The numerical estimates from different factors are calculated in an additive approach by subsequent addition of particular atomic groups (e.g., the sets of H atoms) to the starting structure fragment (e.g., the set of atoms comprising a structural unit). All structure complexity calculations have been performed by means of the TOPOS program package [47].

Chemical complexities of selenium minerals were evaluated by the amount of chemical information per atom ($^{\text{chem}}I_G$) and per formula unit, f.u. ($^{\text{chem}}I_{G,\text{total}}$) [37,38]. Following this approach, for the idealized chemical formula of a mineral or inorganic compound, $E^{(1)}_{c_1}E^{(2)}_{c_2} \dots E^{(k)}_{c_k}$, where $E^{(i)}$ is an i th chemical element in the formula and c_i is its integer coefficient, the chemical information can be calculated as follows:

$$^{\text{chem}}I_G = - \sum_{i=1}^k p_i \log_2 p_i \quad (\text{bits/atom}) \quad (4)$$

$$^{\text{str}}I_G = -e \sum_{i=1}^k p_i \log_2 p_i \quad (\text{bits/cell}) \quad (5)$$

where k is the number of different elements in the formula and p_i is the random choice probability for an atom of the i th element, that is:

$$p_i = c_i/e \quad (6)$$

where e is the total number of atoms in the chemical formula:

$$e = \sum_{i=1}^k c_i \quad (7)$$

For the calculations of chemical complexities, the ideal chemical formulas of minerals were used (see also [37,38]).

3. Results

3.1. Classification of Se Mineral Systems

Our approach allows one to organize mineral species according to their chemical composition and to arrange the existing data in a way complementary to the traditional classification schemes [48–50]. A certain advantage of the new scheme is in its formal and unambiguous character, though we are quite aware that certain amount of essential information is lost. As in all contemporary mineral classifications, Se minerals are divided into five groups: Native selenium, oxide, selenides, selenites (anhydrous, hydrous, and with additional anions) and selenates (anhydrous, hydrous, and with additional anions). Within each of these groups, minerals can be classified according to the minimal number of species-defining elements [28]. According to this value, seven Se mineral systems can be identified, containing from one to seven species-defining elements. Native selenium belongs to the one-component mineral system, whereas minerals containing atoms of two elements only (nevskite, clauthalite, ferroselite, etc.) belong to two-component mineral systems, minerals containing three elements (aguilarite, kawazulite, skippenite, etc.) belong to three-component mineral systems, etc. Our approach allows us to highlight the formulae of “chemically pure” minerals, which contains species-defining elements only. Within this system, each mineral has a unique position defined by its chemical composition. It also makes it easier to apply digital technologies to organize, store, and retrieve thermodynamic data for a particular mineral. The revised classification of Se mineral systems is given in Supplementary Table S2.

3.2. Distribution of Se Minerals According to the Number of Species-Defining Elements

Selenium minerals *sensu stricto* (e.g., minerals with independent crystallographic sites dominated by Se) occur mainly in hydrothermal deposits [51], oxidation zones of ore mineral deposits [40,41], and as products of fumarolic activity [33]. Selenides are also known from magmatic sulfide ores associated with ultrabasic rocks, where they also have a hydrothermal origin.

According to their genesis, Se minerals can be divided into three groups:

- (i) Selenides formed from hydrothermal solutions under relatively reducing conditions;
- (ii) Secondary selenites and selenates, which formation is caused by the activity of aqueous solutions in surface or near-surface environments, mostly in oxidation zones of sulfide and selenide ores, under atmospheric pressure (~1 bar) and seasonal fluctuations of temperature;
- (iii) Anhydrous selenites found in volcanic fumaroles of the Tolbachik volcano, Kamchatka peninsula, Russia. The genetic environment of these minerals is unique and differs essentially from the formation conditions of other selenites and selenates. Fumarolic selenites precipitate from gas phase at high temperatures (300–400 °C), atmospheric pressure, and low partial pressure of water [33].

The average arithmetic means of the number of species-defining elements, chemical (${}^{\text{chem}}I_G$, ${}^{\text{chem}}I_{G,\text{total}}$) and structural (${}^{\text{str}}I_G$, ${}^{\text{str}}I_{G,\text{total}}$) complexities, $\langle \bar{X} \rangle$, have been calculated for the three genetic groups of Se minerals listed above. Student's *t*-test [52] was used for comparing these means. The data obtained show that, at the 0.05 level, the groups (ii) and (iii) are not significantly different. Therefore, according to the value of $\langle \bar{X} \rangle$, all Se minerals belong to two groups: (1) O-free minerals most of which were formed under endogenic conditions (native selenium and selenides) and (2) minerals formed under exogenic conditions as a result of chemical weathering and fumarolic activities (oxide and oxysalts). The data are summarized in Table 1 and presented visually in Figure 2. They show that exogenic minerals are chemically more complex than endogenic ones. The arithmetic mean of species-defining elements in oxygen-free Se minerals is significantly lower ($\bar{X} = 2.81$; $\sigma_{\bar{X}} = 0.09$) than in oxygen-bearing minerals ($\bar{X} = 4.31$; $\sigma_{\bar{X}} = 0.11$). The *t*-test shows that for both groups of minerals the differences of the number of species-defining elements, chemical (${}^{\text{chem}}I_G$, ${}^{\text{chem}}I_{G,\text{total}}$) and structural (${}^{\text{str}}I_G$, ${}^{\text{str}}I_{G,\text{total}}$) complexities are statistically significant with the confidence level of more than 99.99 %.

Table 1. Distribution of Se minerals according to the number of species-defining elements.

N	Selenium Minerals					
	All Selenium Minerals		Selenides and Native Selenium		Oxide, Selenites, and Selenates	
	m_i	p_i	m_i	p_i	m_i	p_i
1	1	0.81	1	1.16	–	–
2	39	31.71	38	44.19	1	2.70
3	38	30.90	35	40.70	3	8.11
4	21	17.07	7	8.14	14	37.85
5	17	13.82	5	5.81	12	32.43
6	5	4.06	–	–	5	13.51
7	2	1.63	–	–	2	5.40
Total	123	100.00	86	100.00	37	100.00

Note: N—the number of the species-defining elements; m —number of minerals; $p_i = (m_i / \sum_{i=1}^7 m_i) \cdot 100$ —probability, %.

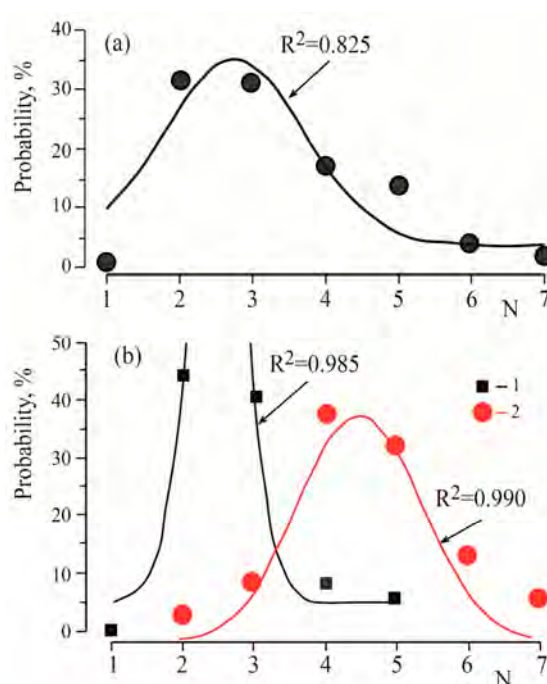


Figure 2. Distribution of Se minerals among mineral systems based on the number of the species-defining elements: (a) all minerals; (b) endogenous (1, black line) and exogenous (2, red line) minerals.

It is worthy to note there are only two mineral species that belong to 7-component systems: carlosruizite, $K_6Na_4Na_6Mg_{10}(SeO_4)_{12}(IO_3)_{12} \cdot 12H_2O$ [53], and prewittite, $KPb_{1.5}ZnCu_6O_2(SeO_3)_2Cl_{10}$ [54]. These two minerals are also most chemically complex among Se minerals with $^{chem}I_{G,total} = 174.7$ and 136.8 bits/formula unit, respectively. All minerals containing six and seven different chemical elements are oxygen-bearing.

The distribution of all selenium minerals versus the number of essential elements, N , is close to normal (Figure 2a) with the determination coefficient $R^2 = 0.825$. The highest number of minerals corresponds to two- and three-component systems (39 and 38 mineral species, respectively). The distributions of Se minerals of the two groups (O-free and O-bearing) depending on the value of N are also normal (Table 1, Figure 2b), which is confirmed by statistical estimations. The number of species-forming elements in minerals varies from 1 to 7, and the maximum number of minerals is formed by 3 and 4 species-forming elements.

3.3. Complexity of Se Minerals

Information-based chemical and structural complexity parameters for Se minerals calculated following the Equations (1)–(7) have been separated into groups according to the number N of different species-defining chemical elements present in the chemical formulas (i.e., into different mineral systems). The mean chemical and structural complexities and associated statistical parameters are given in Table 2. Figure 3 shows distribution of Shannon information amounts among different types of mineral systems. The dependencies of different I_G values from N are best approximated by the use of the following exponential functions (corresponding curves are plotted as black and red lines in Figure 3):

$$^{chem}I_G = 2.187 - 2.2 \times \exp(-N/1.915) \quad (R^2 = 0.994) \tag{8}$$

$$^{str}I_G = 4.140 - 6.989 \times \exp(N/2.033) \quad (R^2 = 0.949) \tag{9}$$

$$^{chem}I_{G,total} = 1.638 \times \exp(N/1.553) \quad (R^2 = 0.990) \tag{10}$$

$$^{str}I_{G,total} = 12.461 \times \exp(N/1.864) \quad (R^2 = 0.899) \tag{11}$$

Table 2. Information-based mean chemical and structural complexities of selenium minerals separated into mineral-system types according to the number N of different chemical elements in the chemical formula *.

N	m_i	$^{chem}I_G$ [bits/atom]			$^{chem}I_{G,total}$ [bits/formula]			m_i	$^{str}I_G$ [bits/atom]			$^{str}I_{G,total}$ [bits/cell]		
		\bar{X}	σ_X	$\sigma_{\bar{X}}$	\bar{X}	σ_X	$\sigma_{\bar{X}}$		\bar{X}	σ_X	$\sigma_{\bar{X}}$	\bar{X}	σ_X	$\sigma_{\bar{X}}$
1	1	0			0			1	0			0		
2	39	1.0	0.04	0.01	4.8	5.4	0.9	28	1.5	0.6	0.1	20.2	30.0	5.7
3	38	1.5	0.1	0.02	12.7	15.4	2.5	19	1.9	0.9	0.2	33.5	47.4	10.9
4	21	1.7	0.1	0.03	29.3	16.1	3.5	14	3.3	0.9	0.2	174.2	165.6	44.2
5	17	1.9	0.1	0.04	45.7	14.6	3.5	8	4.1	0.8	0.3	250.1	212.7	75.2
6	5	1.9	0.1	0.06	70.3	23.2	10.4	4	3.8	0.8	0.4	203.4	44.0	22.0
7	2	2.2	0.2	0.13	155.8	26.8	18.9	2	4.1	0.2	0.1	563.7	92.7	65.6

* m_i = number of minerals taken into account; \bar{X} = arithmetic mean; σ_X = standard deviation; $\sigma_{\bar{X}}$ = standard error of mean.

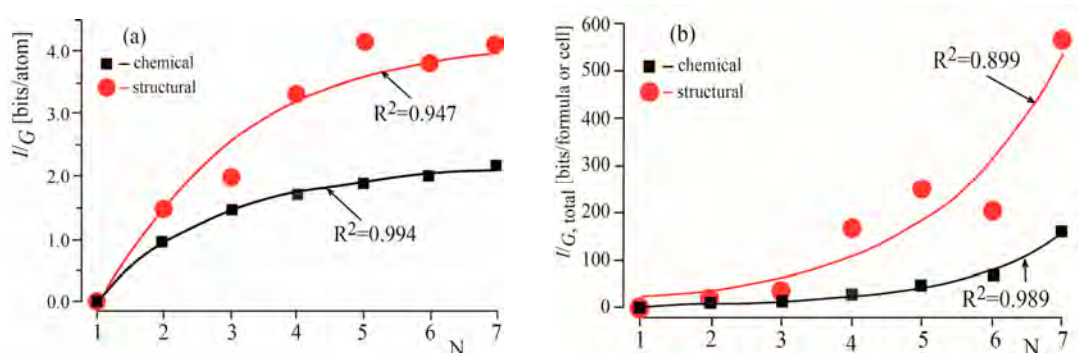


Figure 3. Chemical and structural complexity parameters for minerals plotted against the number N of different chemical elements in a chemical formula (the mineral-system type): Shannon information per atom (a) and per unit cell or formula unit (b).

The observed relations indicate that there is a strong and positive correlation between the chemical and structural complexities and the number of different chemical elements in a mineral. The determination coefficients show that these relations are statistically significant with the confidence level of more than 99%.

Figure 4 shows the relations between the chemical and structural complexities per atom (Figure 4a) and per unit cell or formula (Figure 4b) calculated for different types of Se mineral systems (i.e., minerals

with the same number of chemical elements in a chemical formula). The best fitting for the $^{chem}I_G - ^{str}I_G$ and $^{chem}I_{G,total} - ^{str}I_{G,total}$ relations was obtained by means of the following linear functions:

$$^{str}I_G = -0.250 + 2.018 \times [^{chem}I_G] \quad (R = 0.966) \quad (12)$$

$$^{str}I_{G,total} = 18.449 + 3.502 \times [^{chem}I_{G,total}] \quad (R = 0.971) \quad (13)$$

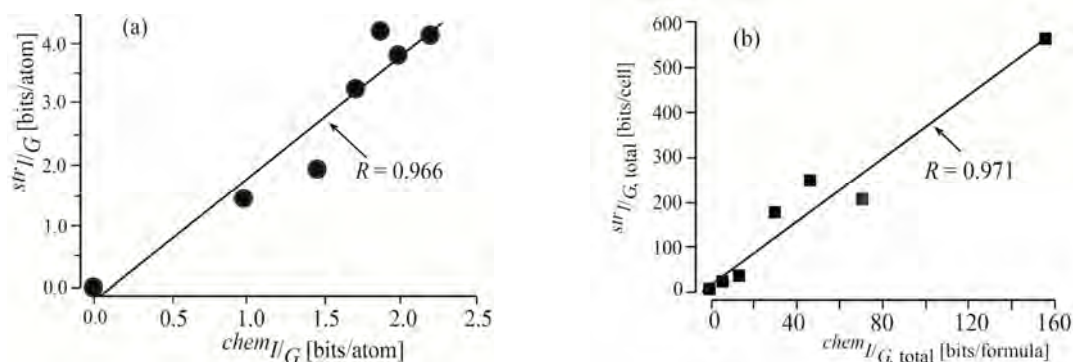


Figure 4. Dependencies between structural and chemical complexities for Se minerals: Shannon information per atom (a) and per unit cell or formula unit (b). Each point corresponds to a particular mineral-system type (or the number N of different elements in a chemical formula).

The observed relationships provide strong evidence that there is an overall trend of increasing structural complexity with increasing chemical complexity of minerals. The correlation coefficients show that these relations are statistically significant with the confidence level of more than 9%.

It is of special interest to compare Se minerals formed in various geochemical environments on the basis of their chemical and structural complexities. Table 3 summarizes data of chemical and structural complexities of two groups of Se minerals formed under (1) endogenic conditions (selenides and native selenium, i.e., O-free minerals) and (2) exogenic conditions as a result of chemical weathering and fumarolic activities (oxide and oxysalts, i.e., O-bearing minerals). Statistical analysis shows that the arithmetic means of chemical and structural complexities per atom and formula/cell for O-free Se minerals are significantly lower than those for O-bearing species. The *t*-test [52] shows that the differences are statistically significant with a confidence level higher than 99.99%.

Table 3. Information-based mean chemical and structural complexities of Se minerals. separated into two groups*.

Complexities	O-Free Minerals				O-Bearing Minerals			
	<i>m</i>	\bar{X}	σ_X	$\sigma_{\bar{X}}$	<i>m</i>	\bar{X}	σ_X	$\sigma_{\bar{X}}$
$^{chem}I_G$ [bits/atom]	87	1.3	0.3	0.03	37	1.8	0.3	0.04
$^{chem}I_{G,total}$ [bits/formula]	87	11.6	14.4	1.6	37	47.0	35.1	5.8
$^{str}I_G$ [bits/atom]	48	1.7	0.8	0.2	21	3.6	0.9	0.2
$^{str}I_{G,total}$ [bits/cell]	48	26.7	40.0	5.8	21	200.2	165.5	36.1

* *m* = number of minerals taken into account; \bar{X} = arithmetic mean; σ_X = standard deviation; $\sigma_{\bar{X}}$ = standard error of mean.

3.4. Most Structurally Complex Se Minerals

Table 4 lists the five most structurally complex Se minerals and provides their total information-based complexity parameters. Figure 5 provides diagrams showing contributions of different crystal chemical factors to the total structural complexity estimated as described in Section 2.2. It is noteworthy that

all the five minerals are O-bearing. Outlined below are basic features of the structural architecture of these minerals with the emphasis on the parameters that control their complexity.

Table 4. Information-based structural complexity parameters for the five most complex Se minerals.

Mineral Name	Code	Chemical Formula	I_G [bits/atom]	$I_{G,total}$ [bits/cell]
Marthozite	Mrz	$\text{Cu}(\text{UO}_2)_3(\text{SeO}_3)_2\text{O}_2 \cdot 8\text{H}_2\text{O}$	5.2	744.5
Mandarinoite	Mnd	$\text{Fe}_2(\text{SeO}_3)_3 \cdot 6\text{H}_2\text{O}$	5.0	640.0
Carlosruizite	Crz	$\text{K}_6\text{Na}_4\text{Na}_6\text{Mg}_{10}(\text{SeO}_4)_{12}(\text{IO}_3)_{12} \cdot 12\text{H}_2\text{O}$	4.0	629.3
Prewittite	Prw	$\text{KPb}_{1.5}\text{ZnCu}_6\text{O}_2(\text{SeO}_3)_2\text{Cl}_{10}$	4.2	498.1
Nicksobolevite	Nsb	$\text{Cu}_7(\text{SeO}_3)_2\text{O}_2\text{Cl}_6$	4.6	420.2

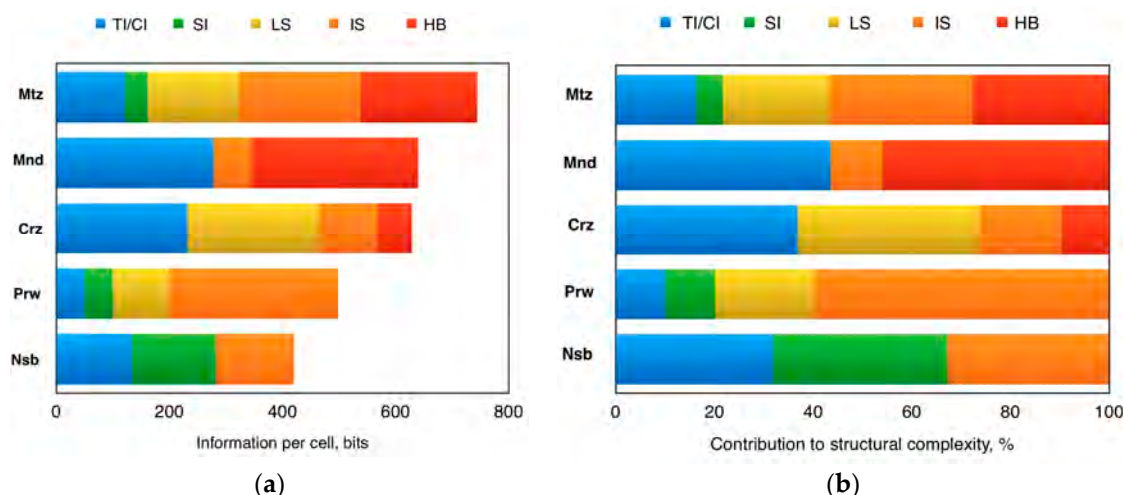


Figure 5. Ladder diagrams showing contributions of various factors to structural complexity: In terms of bits per unit cell (a) and in relative terms (in percent; (b)). Legend for colors: TI = topological information; CI = cluster information (valid for Prw and Nsb: See text for details); SI = structural information; LS = layer stacking; IS = interstitial structure; HB = hydrogen bonding. Legend for minerals see in Table 4.

The most complex Se mineral known so far is marthozite, $\text{Cu}(\text{UO}_2)_3(\text{SeO}_3)_2\text{O}_2 \cdot 8\text{H}_2\text{O}$, first described from the Musonoi mine, Lualaba, Democratic Republic of Congo [55]. Its crystal structure [56] is based upon the $[(\text{UO}_2)_3(\text{SeO}_3)_2\text{O}_2]^{2-}$ uranyl selenite layers formed by edge-sharing (UO_7) and (UO_8) bipyramids (Figure 6). The layers belong to the phosphuranylite anion topology [57] with pentagons and hexagons populated by uranyl cations, $(\text{UO}_2)^{2+}$, and triangles populated by selenite anions, $(\text{SeO}_3)^{2-}$. There are two layers per unit cell linked through Cu^{2+} cations forming bonds to the oxygen atoms of uranyl ions from the adjacent layers. The interlayer space contains H_2O molecules bonded to Cu^{2+} as well as the H_2O molecules held in the structure by hydrogen bonds only.

The layer shown in Figure 6b possesses some interesting features that deserve special consideration. The selenite groups within the layer may have two different orientations relative to the layer plane, i.e., either up (**U**) or down (**D**). Different systems of orientations of selenite groups correspond to different geometrical isomers, which are defined as structural units with identical global but different local topology [58,59]. Figure 7a shows the phosphuranylite anion topology, which consists of hexagons, pentagons, squares, and triangles. In phosphuranylite-type layers, hexagons and pentagons are populated by uranyl ions, triangles are populated either by tetrahedra (for phosphates and arsenates) or triangular pyramids (for selenites), and the squares are empty. Geometrical isomerism of phosphuranylite-type layers was considered in detail in [60], where five different systems of orientations of tetrahedra/pyramids have been distinguished. The simplest geometrical isomer is the **ud/du** isomer shown in Figure 7b (here the **u** and **d** symbols inside triangles symbolize orientations of tetrahedra or triangular pyramidal groups either up or down relative to the plane of the layers,

respectively). It is of interest that this isomer has not been observed in minerals, but is known for synthetic $\text{Sr}[(\text{UO}_2)_3(\text{SeO}_3)_2\text{O}_2] \cdot 4\text{H}_2\text{O}$ [61]. Its topological complexity (i.e., complexity of its most symmetrical version) is equal to 3.1 bits/atom and 58.7 bits/cell. The layer in marthozite belongs to the **ud/ud** isomer (Figure 7c), which is the most common in minerals (see [60] for references). Its topological complexity is higher than that of the **ud/du** isomer and equals to 3.2 bits/atom and 121.4 bits/cell. However, in the real crystal structure, the symmetry of the layer is far from ideal, and the structural complexity of the layer is equal to 4.2 bits/atom and 161.4 bits/cell. In general, the high complexity of the crystal structure of marthozite is the sum of four almost equal contributions (Figure 5b): Structural complexity of the uranyl selenite layer (21.6%), layer stacking (21.6% as there are two layers per unit cell), interstitial structure (29.0%: Cu^{2+} cations and interlayer H_2O groups), and hydrogen atoms (26.6%).

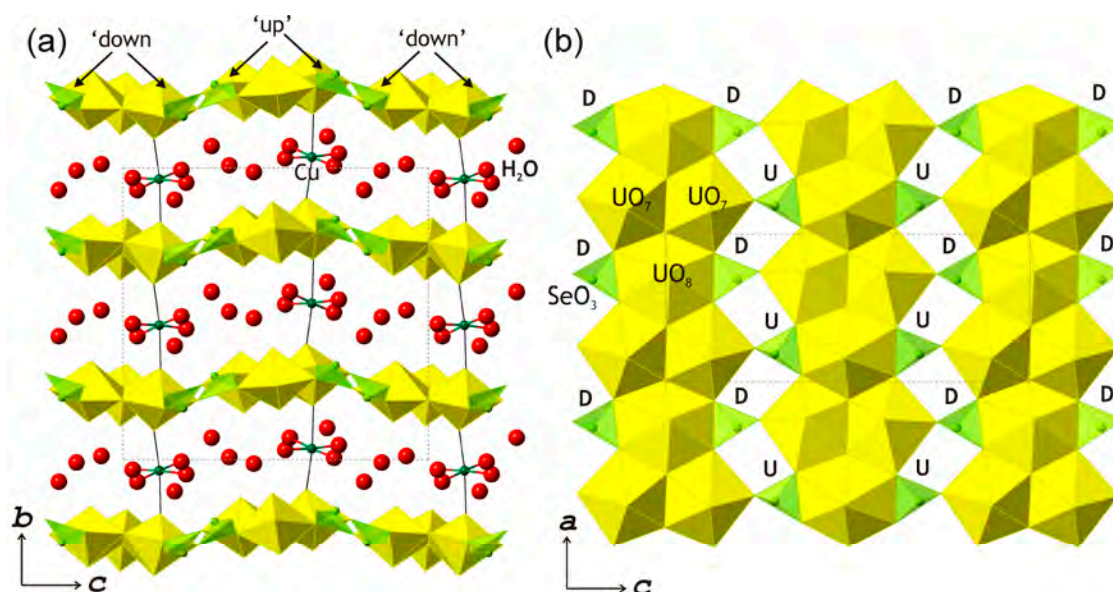


Figure 6. The crystal structure of marthozite projected along the a axis (a) and the projection of the uranyl selenite layer (b). The U and D symbols in (b) indicate orientation of (SeO_3) pyramids up and down relative to the plane of the layer, respectively. See text for details.

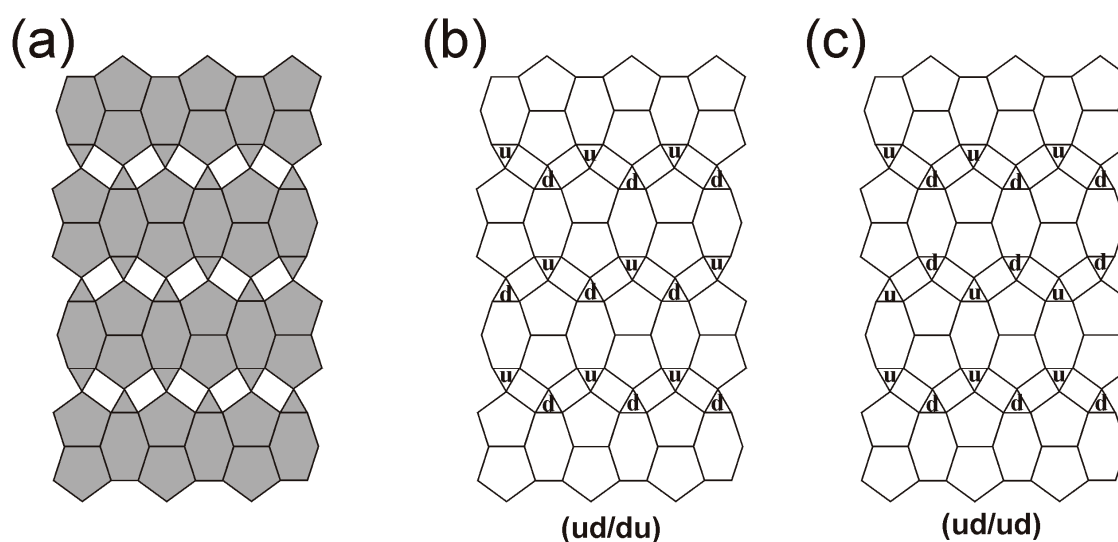


Figure 7. The phosphuranylite anion topology (a), the simplest geometrical isomer **ud/du** (b) and the **ud/ud** isomer (c) realized in the crystal structure of marthozite. See text for details.

The second most structurally complex Se mineral is mandarinoite, $\text{Fe}_2(\text{SeO}_3)_3 \cdot 6\text{H}_2\text{O}$, that was first described as an alteration product of penroseite, NiSe_2 , at Pacajake mine near Hiaco, Colquechaca, Bolivia [62], and later found at other localities worldwide [63–66]. Its crystal structure was solved by Hawthorne [67], who defined it as a hexahydrate. However, this conclusion was recently questioned by Holzheid et al. [68], who suggested for mandarinoite the chemical formula $\text{Fe}_2(\text{SeO}_3)_3 \cdot (6-x)\text{H}_2\text{O}$ ($x = 0-1$) with variable H_2O content. The synthetic analogue of mandarinoite with $x = 1$, $\text{Fe}_2(\text{SeO}_3)_3 \cdot 5\text{H}_2\text{O}$, was investigated recently by Lelet et al. [69]. The Te analogue of the mineral, telluromandarinoite, $\text{Fe}_2(\text{SeO}_3)_3 \cdot 6\text{H}_2\text{O}$, was described by Back et al. [70]. The crystal structure of the mineral [67] consists of a microporous framework formed by corner sharing of $(\text{Fe}\varphi_6)$ octahedra ($\varphi = \text{O}, \text{H}_2\text{O}$) and SeO_3 pyramids (Figure 8a). The framework channels accommodate H_2O molecules not bonded to Fe^{3+} cations.

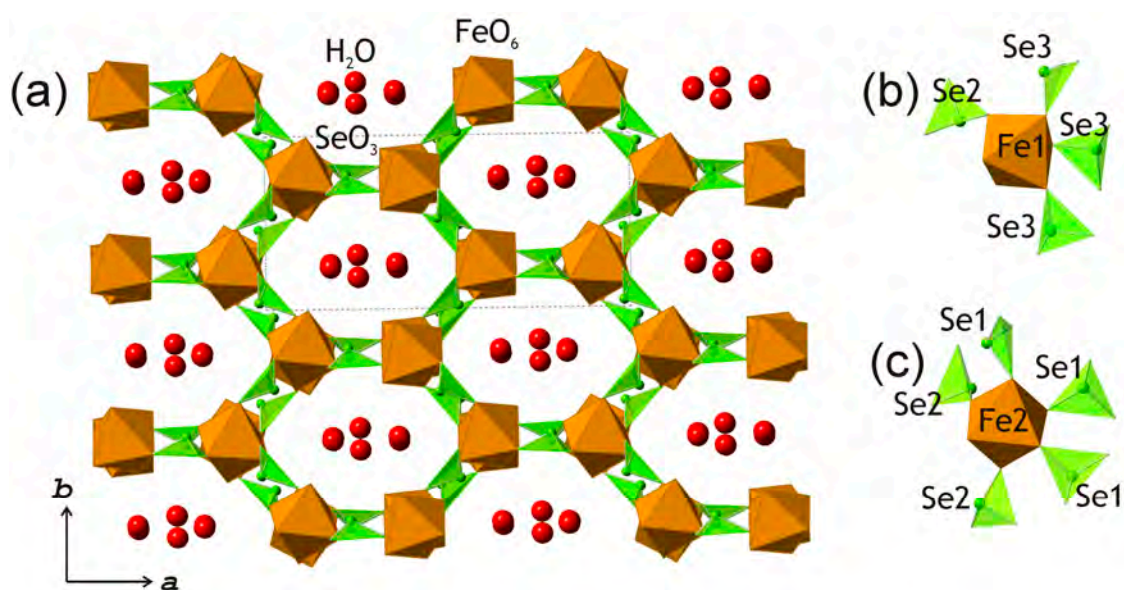


Figure 8. The crystal structure of mandarinoite projected along the c axis (a) and local coordination of Fe1 (b) and Fe2 (c) sites.

The topology of the iron selenite hydrate framework is rather complex. There are two symmetrically independent Fe sites with different local coordination environments (Figure 8b,c). The Fe1 site is coordinated by four O atoms of selenite groups and two H_2O molecules in a *cis*-arrangement (Figure 8b), whereas the Fe2 site is coordinated by five O atoms of selenite groups and one H_2O molecule (Figure 8c). The topology of the framework can better be described using a nodal approach, where coordination polyhedra of Fe and Se atoms are replaced by nodes, and the linkage of two adjacent nodes means that the respective polyhedra share a common oxygen atom. This approach is quite efficient for the description and understanding topology of complex layered and framework heteropolyhedral structures [60,71,72].

The nodal representation of the topology of mandarinoite heteropolyhedral framework is shown in Figure 9a. It can be described as consisting of layers parallel to the (100) plane (Figure 9b) interlinked by planar chains running along the c axis with their planes parallel to (010) (Figure 9c). The topology of the layers is common for inorganic oxysalts and consists of four- and eight-membered rings (Figure 9d) [60,72]. The chains consist of 3-connected Se2 nodes and correspond to the branched *zweier* chains (Figure 9e). The chains have different orientations along the a axis, which results in the different valencies of the Fe1 and Fe2 nodes (four and five, respectively).

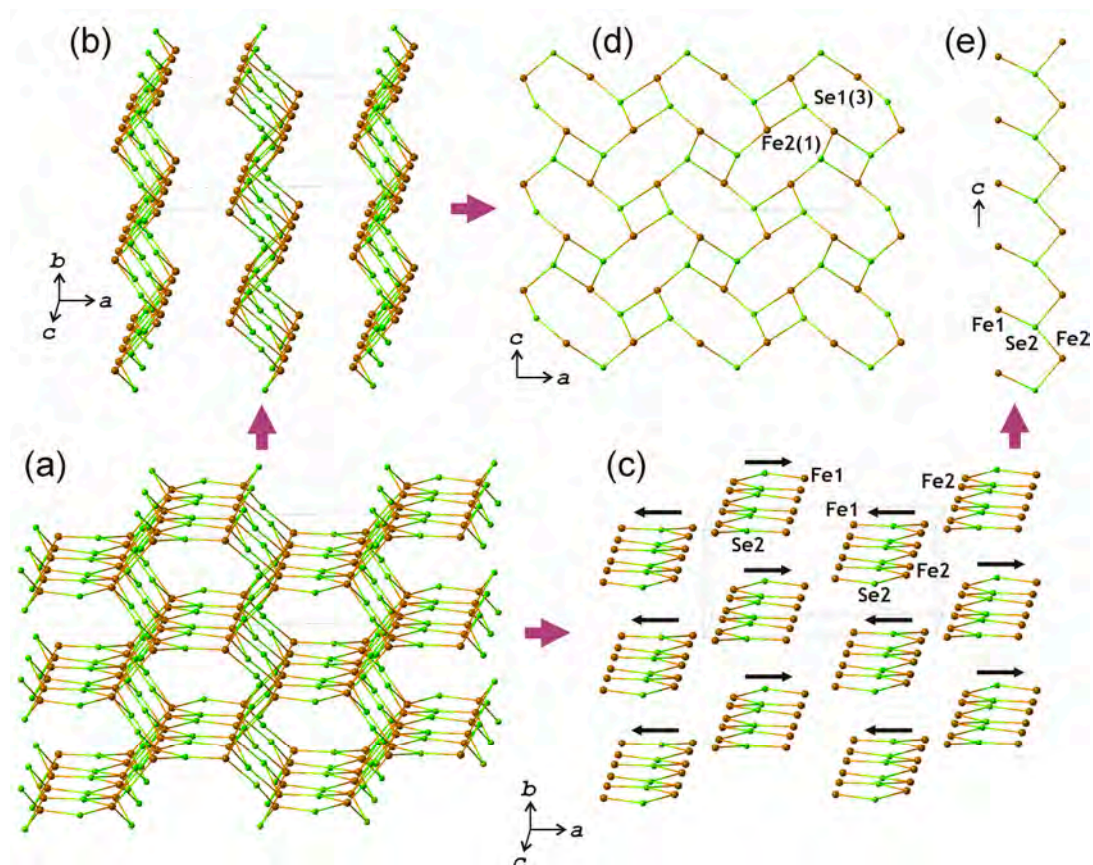


Figure 9. The nodal representation of the topology of the iron selenite hydrate framework in the crystal structure of mandarinoite (a) can be split into the sequence of layers (b) interlinked by the system of chains (c). The topology of the layers consists of eight- and four-membered rings (d), whereas the topology of the chains is of simple branched type (e). Black arrows in (c) indicate orientations of the chains along the *a* axis.

Figure 5b shows that the overall structural complexity of mandarinoite is due to the two major contributions: Framework complexity (43.4%) and hydrogen bonding (46.1%) with a smaller contribution from the interstitial H₂O groups (10.5%).

As it was mentioned above, carlosruizite, K₆Na₄Na₆Mg₁₀(SeO₄)₁₂(IO₃)₁₂·12H₂O [53], is the most chemically complex Se mineral that was found as a saline mineral in Chilean nitrate fields. Yet, its structural complexity ranks as third after marthozite and mandarinoite. The crystal structure of the mineral is trigonal and is based upon the complex five-level layers of corner-sharing (Mgφ₆) octahedra (φ = O, H₂O), IO₃ pyramids and SeO₄ tetrahedra (Figure 10a). The layers are parallel to the (001) plane (Figure 10b). The fundamental building block (FBB) of the layer (Figure 10c) consists of two octahedra linked by three IO₃ pyramids. One of the octahedra (upper in Figure 10c) shares its three corners with three adjacent selenate groups, whereas the second octahedron (lower in Figure 10c) contains three H₂O groups. The adjacent FBBs are linked via additional (Mgφ₆) octahedra located in between them by sharing non-shared corners of the IO₃ pyramids. The K⁺ and Na⁺ cations are located in the interlayer space providing, along with hydrogen bonds, the three-dimensional integrity of the crystal structure.

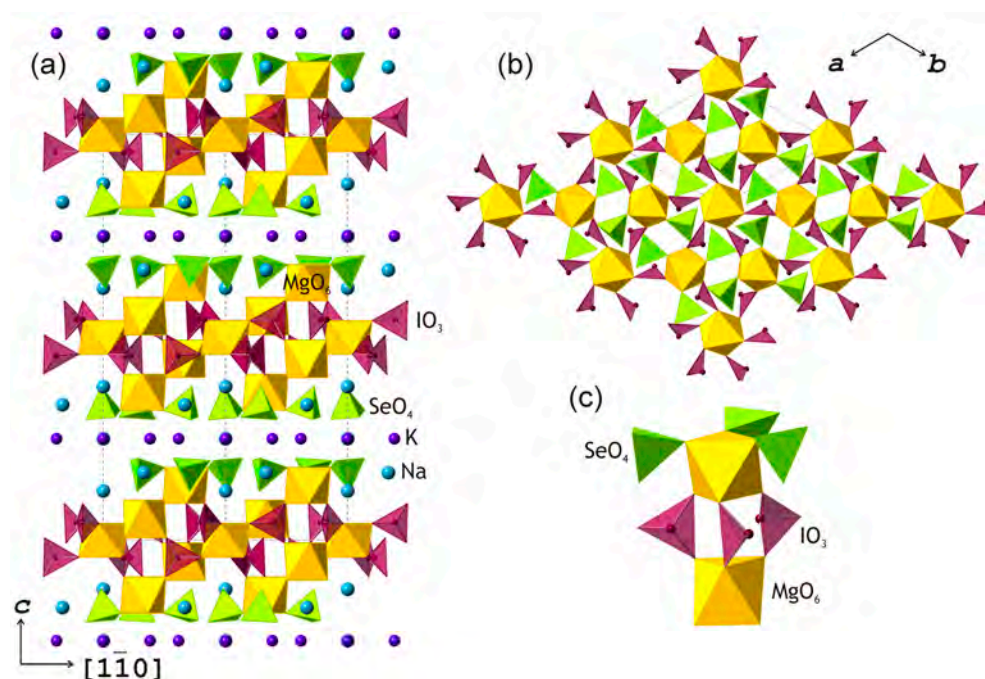


Figure 10. The crystal structure of carlosruizite projected along [110] (a), the projection of the Mg-iodate-selenate-hydrate layer (b), and the fundamental building block of the layer (c).

The overall structural complexity of carlosruizite is dominated by the contributions from the topological complexity of the layers (36.9%) and layer stacking (36.9%; there are two layers per cell), with smaller contributions from interstitial structure (16.5%) and hydrogen atoms (9.7%). The high topological complexity of the layers is obviously influenced by its chemical complexity as it contains three chemically distinct types of coordination polyhedra.

Prewittite, $\text{KPb}_{1.5}\text{ZnCu}_6\text{O}_2(\text{SeO}_3)_2\text{Cl}_{10}$ [54], also has a remarkable chemical complexity containing seven different chemical elements as mineral-defining components. The mineral was found in fumaroles of the Great Fissure Tolbachik eruption (1975–1976, Kamchatka peninsula, Russia), where it crystallized in a high-temperature anhydrous environment directly from volcanic gases. As for other Cu selenite oxide chlorides of fumarolic origin [73], the crystal structure of prewittite can be conveniently described in terms of oxocentered (OM_4) tetrahedra ($\text{M} = \text{metal}$) formed around additional oxygen atoms not bonded to Se. This approach has proved its efficiency in description of complex inorganic structures that are hardly understood from the viewpoint of cation-centered interpretation [74].

In prewittite, two heterometallic ($\text{OCu}_{4-x}\text{Pb}_x$) tetrahedra share a common edge to form dimers shown in Figure 11a. The dimers are attached to two SeO_3 groups that are attached to the faces of the oxocentered tetrahedra in a face-to-face fashion [75], which is typical for the structures of fumarolic minerals and their synthetic analogues based upon anion-centered tetrahedra. The association of oxocentered dimers and selenite groups results in the formation of the $\{[\text{O}_2\text{Cu}_6](\text{SeO}_3)_2\}^{4+}$ clusters (the Cu-Pb disorder is neglected for generality) with the ideal complexity of 2.6 bits/atom and 42.0 bits/cluster. In the real crystal structure, its symmetry is lower than the ideal one and the complexity increases to 3.1 bits/atom and 50.0 bits/cluster. The clusters are linked through additional Cu-O bonds to form layers parallel to (010) (Figure 11b). These metal-oxide layers represent the most strongly bonded atomic arrangements in the crystal structure and are separated by K^+ , Pb^{2+} , Zn^{2+} , and Cl^- ions (Figure 11c). There are two layers per unit cell.

Figure 5b shows that the dominating contribution to the structural complexity of prewittite comes from the complexity of interstitial structure (59.84%), obviously strongly influenced by its complex chemistry, with smaller contributions from cluster information (10.04%), structural information (10.04%), and layer stacking (20.08%; There are two layers per unit cell).

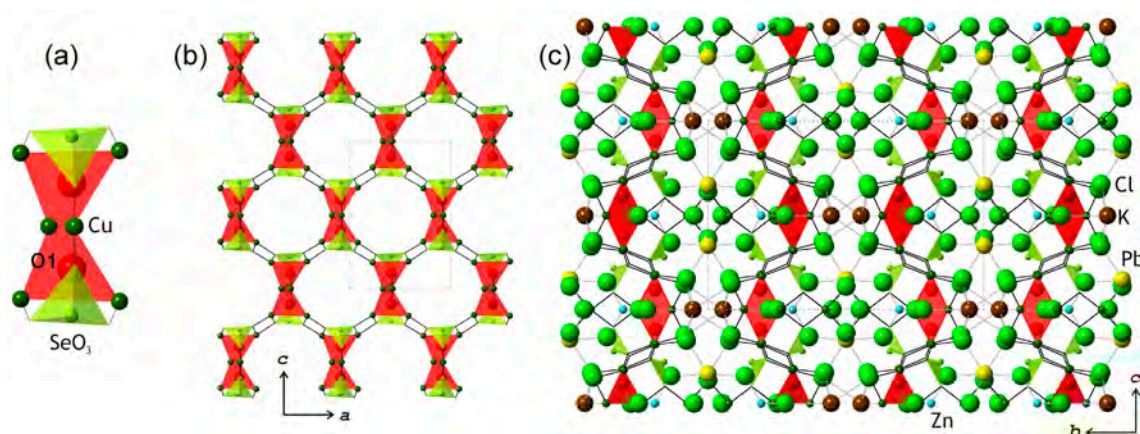


Figure 11. The $\{[O_2Cu_6](SeO_3)_2\}^{4+}$ clusters in the crystal structure of prewittite (the low-occupied Pb sites are omitted for clarity) (a), their linkage into two-dimensional metal-oxide layers (b), and the projection of the whole crystal structure along the a axis (c).

In contrast to prewittite, nicksobolevite, $Cu_7O_2(SeO_3)_2Cl_6$ [76], is chemically more simple and belongs to the 4-component $OClSeCu$ mineral system (three other members of this system are georbokiite, $\alpha-Cu_5O_2(SeO_3)_2Cl_2$ [77], parageorgbokiite, $\beta-Cu_5O_2(SeO_3)_2Cl_2$ [78], and chloromenite, $Cu_9O_2(SeO_3)_4Cl_6$ [79]). However, despite its chemical simplicity, the crystal structure of nicksobolevite is far from being simple. Its FBB is the $\{[O_4Cu_{13}](SeO_3)_4\}^{10+}$ tetramer shown in Figure 12a. The tetramer is formed by four $(O_aCu_4)^{6+}$ tetrahedra linked sequentially by corner sharing and attached to SeO_3 pyramids in the same face-to-face fashion as observed in prewittite (O_a = additional O atoms not bonded to Se). The complexity of the cluster is rather high (4.1 bits/atom and 134.5 bits/cluster), as its length is 13 Å, approaching the nanoscale level. The FBBs are linked via Cu-O bonds and additional Cu^{2+} cations into complex ladder-like layers with the composition $\{Cu[O_4Cu_{13}](SeO_3)_4\}^{10+}$. The layers are stacked along the a axis (Figure 13a) and separated by Cl^- anions (Figure 13b). The structural complexity of nicksobolevite is the sum of contributions from cluster complexity (31.90%), layer complexity (35.24%), and interlayer structure consisting of Cl^- anions only (32.86%).

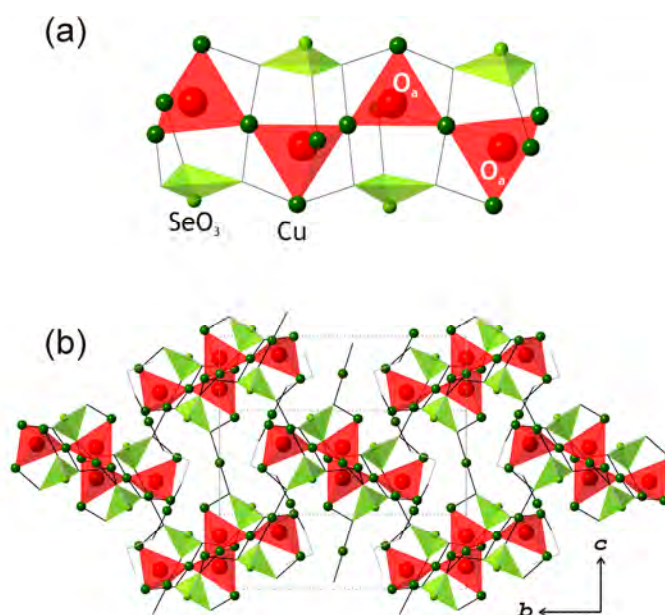


Figure 12. The $\{[O_4Cu_{13}](SeO_3)_4\}^{10+}$ tetramer in the crystal structure of nicksobolevite (a) and the projection of the $\{Cu[O_4Cu_{13}](SeO_3)_4\}^{10+}$ layer perpendicular to the (100) plane (b).

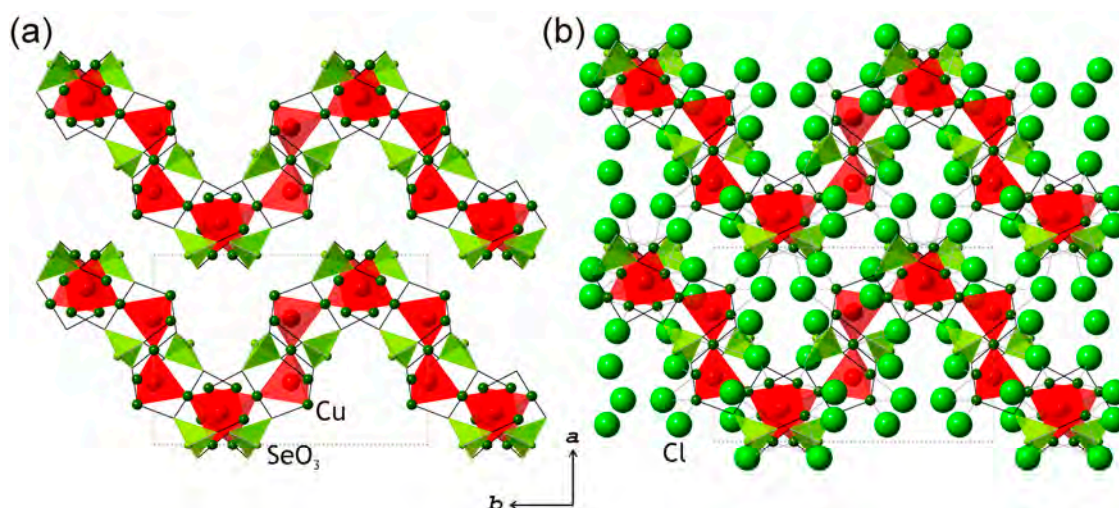


Figure 13. The stacking of the ladder-like $\{\text{Cu}[\text{O}_4\text{Cu}_{13}](\text{SeO}_3)_4\}^{10+}$ layers in nicksobolevite (a) and the whole structure projected along the c axis (b).

The high structural complexity of both prewittite and nicksobolevite originates in part from the presence of the high amount of chloride ions in the crystal structure. The occurrence of copper selenite chlorides in Tolbachik fumaroles and their relative stability in anhydrous environments are in part the result of the presence of attractive closed-shell interactions between Se^{4+} ions of selenite groups and Cl^- anions recently investigated by means of density functional theory (DFT) calculations [80].

4. Discussion

The average structural complexity of Se minerals is equal to 2.4(1) bits/atom and 101(17) bits/cell. This is less than the average structural complexity for all minerals identified by S. Krivovichev [23] as 3.2(2) bits/atom and 228(6) bits/cell. However, if we consider O-bearing Se minerals only, their average complexity is close to that for all minerals, 3.6(2) bits/atom and 200(36) bits/cell. The O-free Se minerals are remarkably less complex than the O-bearing species, owing to their primary character. Their average structural complexity parameters are equal to 1.7(2) bits/atom and 27(6) bits/cell.

It is of interest to compare the complexity of O-bearing Se minerals with other chemical groups, e.g., with borate minerals, for which Grew et al. [30] reported the average complexity per unit cell equal to 340 bits. It should be noted that, according to the classification proposed in [23], there are no very complex Se minerals with >1000 bits/cell. All five most complex Se minerals listed in Table 4 belong to the groups of intermediate (100–500 bits) or complex (500–1000 bits) structures. In contrast, among 259 structures of B minerals, eight (3%) are very complex, i.e., with the $^{\text{str}}I_{G,\text{total}}$ value exceeding 1000 bits. The difference in complexity between the O-bearing B and Se minerals arises from the number of factors, three of which are listed below.

1. Boron does not occur in nature as borides, whereas Se forms a large diversity of selenides with relatively low structural complexity. The only known O- and F-free boron mineral is qingsongite, BN, which possesses a diamond-type structure with $^{\text{str}}I_{G,\text{total}} = 2$ bits/cell.

2. B^{3+} ions may occur in both tetrahedral and triangular coordinations. In contrast, Se^{6+} occurs in exclusively tetrahedral coordination, but Se^{6+} is unstable and easily transforms into Se^{4+} ions [41], which possess a trigonal pyramidal coordination, forming stable $(\text{Se}^{4+}\text{O}_3)^{2-}$ ions.

3. $(\text{B}^{3+}\text{O}_3)^{3-}$ and $(\text{B}^{3+}\text{O}_4)^{5-}$ polymerize to form borate polyanions with variable topologies and dimensionalities, whereas $(\text{Se}^{4+}\text{O}_3)^{2-}$ ions do not polymerize easily. There are no oxysalt minerals that contain polymerized $(\text{Se}^{4+}\text{O}_3)^{2-}$ groups, though such structures are known for synthetic compounds (see, e.g., [81]).

Therefore, in contrast to borates, structurally complex Se minerals owe their complexity not to the formation of complex polymerized selenite, selenate or selenite-selenate structural units, but to the

leading role of other factors. In marthozite, the leading role belongs to the uranyl ions, which, along with isolated selenite groups, form condensed layers responsible for ~50% of structural information with the rest of information coming from interstitial structure including hydrogen atoms of H₂O molecules. The high structural complexity of uranyl minerals is not surprising: The most structurally complex mineral known today is ewingite, Mg₈Ca₈(UO₂)₂₄(CO₃)₃₀O₄(OH)₁₂(H₂O)₁₃₈ [82]. In mandarinoite, structural complexity results mostly from the complexity of the microporous framework formed by Fe and Se polyhedra with additional considerable contribution from the high hydration state. Structural complexities of carlosruizite and prewittite are controlled by their high chemical complexities that define the high topological complexity of layers in the first and the high complexity of interlayer structure in the second. Finally, the complexity of nicksobolevite is the result of the high complexity of its anion-centered substructure and the high Cl content. In most cases, selenium itself does not play the crucial role in determining structural complexity (there are structural analogues or close species of marthozite, mandarinoite, and carlosruizite that do not contain Se), except for selenite chlorides, where stability of crystal structures is adjusted by the existence of attractive Se ⋯ Cl closed-shell interactions impossible for sulfates or phosphates. Thus, the presence of lone-pair electrons on Se⁴⁺ anions has some influence upon the overall complexity of natural copper selenite chlorides [79].

Finally, most structurally complex Se minerals originate either from relatively low-temperature hydrothermal environments (as marthozite, mandarinoite, and carlosruizite) or from mild (500–700 °C) anhydrous gaseous environments of volcanic fumaroles. In general, the average complexities of these two groups do not differ significantly since both are composed from minerals with relatively low and relatively high complexity parameters.

Supplementary Materials: The following are available online at <http://www.mdpi.com/2075-163X/9/7/455/s1>, Table S1: Selenium's minerals: Chemical formula, type locality (TL) and number of localities (NL), Table S2: Classification of mineral systems of selenium minerals.

Author Contributions: Conceptualization, V.G.K., S.V.K.; methodology, V.G.K., S.V.K. and M.V.C.; investigation, V.G.K., S.V.K. and M.V.C.; writing—original draft preparation, V.G.K. and S.V.K.; writing—review and editing, V.G.K., S.V.K. and M.V.C.

Funding: This research was funded by the Russian Science Foundation (grant 19-17-00038 for the complexity part and 18-17-00018 for the part on uranyl selenites).

Acknowledgments: We are grateful to the reviewers for their constructive and insightful remarks.

Conflicts of Interest: The authors declare no conflicts of interest.

References

1. Hazen, R.M.; Grew, E.S.; Downs, R.T.; Golden, J.; Hystad, G. Mineral ecology: Chance and necessity in the mineral diversity of terrestrial planets. *Can. Mineral.* **2015**, *53*, 295–324. [CrossRef]
2. Hazen, R.M.; Hystad, G.; Golden, J.J.; Hummer, D.R.; Liu, C.; Downs, R.T.; Morrison, S.M.; Grew, E.S. Cobalt mineral ecology. *Am. Mineral.* **2017**, *102*, 108–116. [CrossRef]
3. Liu, C.; Hystad, G.; Golden, J.J.; Hummer, D.R.; Downs, R.T.; Morrison, S.M.; Ralph, J.P.; Hazen, R.M. Chromium mineral ecology. *Am. Mineral.* **2017**, *102*, 612–619. [CrossRef]
4. Vernadsky, V.I. *History of the Minerals of the Earth's Crust*; Nauchnoe Khimiko-Tekhnicheskoe Izdatelstvo: Petrograd, Russia, 1923; Volume 1, 209p. (In Russian)
5. Fersman, A.E. On the number of mineral species. *Dokl. AN SSSR* **1938**, *19*, 271–274. (In Russian)
6. Saukov, A.A. On the reason of the restricted number of mineral species. In *Problems of Mineralogy, Geochemistry and Petrography*; Academy of Science of the USSR: Moscow, Leningrad, Russia, 1946; pp. 209–218. (In Russian)
7. Povarennykh, A.S. On the occurrence of chemical elements in the Earth's crust and the number of mineral species. *Mineral. Sb. Lvov Gos. Univ.* **1966**, *20*, 179–185. (In Russian)
8. Urusov, V.S. Why there are only two thousands of them? *Priroda* **1983**, *10*, 82–88. (In Russian)
9. Urusov, V.S. Symmetry statistics of mineral species and evolutionary dissymmetrization of mineral substance. *Zap. Ross. Mineral. Obshch.* **2006**, *135*, 1–12. (In Russian)

10. Ivanov, V.V.; Yushko-Zakharova, O.E. The relations between the occurrence of chemical elements and the number of their minerals in the continental Earth's crust. *Dokl. AN SSSR* **1989**, *308*, 448–451. (In Russian)
11. Khomyakov, A.P. Why there are more than two thousands of them? *Priroda* **1996**, *5*, 62–74. (In Russian)
12. Yaroshevsky, A.A. Number of minerals of different chemical elements: Statistics and some regularities. *Zap. Ross. Mineral. Obshch.* **2003**, *132*, 3–16. (In Russian)
13. Hazen, R.M. Data-driven abductive discovery in mineralogy. *Am. Mineral.* **2014**, *99*, 2165–2170. [[CrossRef](#)]
14. Morrison, S.M.; Liu, C.; Eleish, A.; Prabhu, A.; Li, C.; Ralph, J.; Downs, R.T.; Golden, J.J.; Fox, P.; Hummer, D.R.; et al. Network analysis of mineralogical systems. *Am. Mineral.* **2017**, *102*, 1588–1596. [[CrossRef](#)]
15. Liu, C.; Eleish, A.; Hystad, G.; Golden, J.J.; Downs, R.T.; Morrison, S.M.; Hummer, D.R.; Ralph, J.P.; Fox, P.; Hazen, R.M. Analysis and visualization of vanadium mineral diversity and distribution. *Am. Mineral.* **2018**, *103*, 1080–1086. [[CrossRef](#)]
16. Hazen, R.M.; Downs, R.T.; Eleish, A.; Fox, P.; Gagné, O.C.; Golden, J.J.; Grew, E.S.; Hummer, D.R.; Hystad, G.; Krivovichev, S.V.; et al. Data-Driven Discovery in Mineralogy: Recent Advances in Data Resources, Analysis, and Visualization. *Engineering* **2019**, *5*, 397–405. [[CrossRef](#)]
17. Yushkin, N.P. Evolutionary ideas in modern mineralogy. *Zap. Vses. Mineral. Obshch.* **1982**, *116*, 432–442. (In Russian)
18. Petrov, T.G. On the measure of complexity of geochemical systems from the viewpoint of information theory. *Dokl. AN SSSR* **1970**, *191*, 924–926. (In Russian)
19. Bulkin, G.A. *Introduction to Statistical Geochemistry. Application of Information Theory to Geochemistry*; Nedra: Leningrad, Russia, 1972; 208p. (In Russian)
20. Bulkin, G.A. Complexity of geochemical systems and their equilibrium. *Dokl. AN SSSR* **1972**, *204*, 956–959. (In Russian)
21. Yushkin, N.P. *Theory and Methods of Mineralogy*; Nauka: Leningrad, Russia, 1977. (In Russian)
22. Krivovichev, S.V. Topological complexity of crystal structures: Quantitative approach. *Acta Crystallogr.* **2012**, *A68*, 393–398. [[CrossRef](#)]
23. Krivovichev, S.V. Structural complexity of minerals: Information storage and processing in the mineral world. *Mineral. Mag.* **2013**, *77*, 275–326. [[CrossRef](#)]
24. Krivovichev, S.V. Which inorganic structures are the most complex? *Angew. Chem. Int. Ed.* **2014**, *53*, 654–661. [[CrossRef](#)]
25. Krivovichev, S.V. Structural complexity of minerals and mineral parageneses: Information and its evolution in the mineral world. In *Highlights in Mineralogical Crystallography*; Danisi, R., Armbruster, T., Eds.; Walter de Gruyter GmbH: Berlin, Germany; Boston, MA, USA, 2015; pp. 31–73.
26. Krivovichev, S.V. Ladders of information: What contributes to the structural complexity in inorganic crystals. *Z. Kristallogr.* **2018**, *233*, 155–161. [[CrossRef](#)]
27. Krivovichev, S.V. Structural complexity and configurational entropy of crystalline solids. *Acta Crystallogr.* **2016**, *B72*, 274–276.
28. Krivovichev, V.G.; Charykova, M.V. *Classification of Mineral Systems*; St.-Petersburg University Press: Saint-Petersburg, Russia, 2013; 196p. (In Russian)
29. Krivovichev, V.G.; Charykova, M.V. Number of Minerals of Various Chemical elements: Statistics 2012 (a New Approach to an Old Problem). *Zap. Ross. Mineral. Obshch.* **2013**, *142*, 36–42, (In Russian; English translation: *Geol. Ore Deposits* **2014**, *56*, 553–559). [[CrossRef](#)]
30. Grew, E.S.; Krivovichev, S.V.; Hazen, R.M.; Hystad, G. Evolution of structural complexity in boron minerals. *Can. Mineral.* **2016**, *54*, 125–143. [[CrossRef](#)]
31. Krivovichev, V.G.; Charykova, M.V. Mineral Systems, Their Types, and Distribution in Nature. I. Khibiny, Lovozero, and the Mont Saint-Hilaire. *Zap. Ross. Mineral. Obshch.* **2015**, *144*, 1–12, (In Russian; English translation: *Geol. Ore Deposits* **2016**, *58*, 551–558). [[CrossRef](#)]
32. Krivovichev, V.G.; Charykova, M.V. Mineral and Physicochemical Systems of Evaporites: Geochemical and Thermodynamic Aspects. *Zap. Ross. Mineral. Obshch.* **2016**, *145*, 30–43, (In Russian; English translation: *Geol. Ore Deposits* **2017**, *59*, 575–583). [[CrossRef](#)]
33. Krivovichev, V.G.; Charykova, M.V. Mineral Systems, Their Types, and Distribution in Nature: 2. Products of Contemporary Fumarole Activity at Tolbachik Volcano (Russia) and Vulcano (Italy). *Zap. Ross. Mineral. Obshch.* **2017**, *146*, 15–28, (In Russian; English translation: *Geol. Ore Deposits* **2017**, *59*, 677–686).

34. Krivovichev, V.G.; Charykova, M.V. Mineral Systems, Their Types, and Distribution in Nature: 3. Otto Mountain (USA) and Dragon (Bolivia) Deposits. *Zap. Ross. Mineral. Obshch.* **2018**, *147*, 14–27. (In Russian)
35. Hazen, R.M.; Papineau, D.; Bleeker, W.; Downs, R.T.; Ferry, J.M.; McCoy, T.J.; Sverjensky, D.A.; Yang, H. Mineral evolution. *Am. Mineral.* **2008**, *93*, 1693–1720. [[CrossRef](#)]
36. Hazen, R.M. Paleomineralogy of the Hadean Eon: A preliminary species list. *Am. J. Sci.* **2013**, *313*, 807–843. [[CrossRef](#)]
37. Krivovichev, V.G.; Charykova, M.V.; Krivovichev, S.V. The concept of mineral systems and its application to the study of mineral diversity and evolution. *Eur. J. Mineral.* **2018**, *30*, 219–230. [[CrossRef](#)]
38. Krivovichev, S.V.; Krivovichev, V.G.; Hazen, R.M. Structural and chemical complexity of minerals: Correlations and time evolution. *Eur. J. Mineral.* **2018**, *30*, 231–236. [[CrossRef](#)]
39. Pasero, M. The New IMA List of Minerals. 2019. Available online: <http://ima-cnmnc.nrm.se/imalist.htm> (accessed on 22 July 2019).
40. Charykova, M.V.; Krivovichev, V.G. Mineral systems and the thermodynamics of selenites and selenates in the oxidation zone of sulfide ores—A review. *Mineral. Petrol.* **2017**, *111*, 121–134. [[CrossRef](#)]
41. Krivovichev, V.G.; Charykova, M.V.; Vishnevsky, A.V. The thermodynamics of selenium minerals in near-surface environments. *Minerals* **2017**, *7*, 188. [[CrossRef](#)]
42. Hawthorne, F.C. The use of end-member charge-arrangements in defining new mineral species and heterovalent substitutions in complex minerals. *Can. Mineral.* **2002**, *40*, 699–710. [[CrossRef](#)]
43. Hatert, F.; Burke, E.A.J. The IMA-CNMNC dominant-constituent rule revised and extended. *Can. Mineral.* **2008**, *46*, 717–728. [[CrossRef](#)]
44. Nikolaev, S.M. *Statistika Sovremennoi Mineralogicheskoi Informatsii (Statistics of Modern Mineralogical Information)*, 2nd ed.; Academic Publishing House “GEO”: Novosibirsk, Russia, 2009; 128p. (In Russian)
45. Pankova, Y.A.; Gorelova, L.A.; Krivovichev, S.V.; Pekov, I.V. The crystal structure of ginorite, $\text{Ca}_2[\text{B}_{14}\text{O}_{20}(\text{OH})_6](\text{H}_2\text{O})_5$, and the analysis of dimensional reduction and structural complexity in the $\text{CaO-B}_2\text{O}_3\text{-H}_2\text{O}$ system. *Eur. J. Mineral.* **2018**, *30*, 277–287. [[CrossRef](#)]
46. Gurzhiy, V.V.; Plasil, J. Structural complexity of natural uranyl sulfates. *Acta Crystallogr.* **2019**, *B75*, 39–48. [[CrossRef](#)]
47. Blatov, V.A.; Shevchenko, A.P.; Proserpio, D.M. Applied topological analysis of crystal structures with the program package ToposPro. *Cryst. Growth Des.* **2014**, *14*, 3576–3586. [[CrossRef](#)]
48. Mills, S.J.; Hatert, F.; Nickel, E.H.; Ferraris, G. The standardisation of mineral group hierarchies: Application to recent nomenclature proposals. *Eur. J. Mineral.* **2009**, *21*, 1073–1080. [[CrossRef](#)]
49. Bulakh, A.G.; Zolotarev, A.A.; Krivovichev, V.G. *Structures, Isomorphism, Formulae, Classification of Minerals*; St.-Petersburg University Press: Saint-Petersburg, Russia, 2014; 133p. (In Russian)
50. Strunz, H.; Nickel, E.H. *Strunz Mineralogical Tables*, 9th ed.; Schweizerbart’sche Verlagsbuchhandlung: Berlin/Stuttgart, Germany, 2001; 870p.
51. Grundmann, G.; Förster, H.-J. Origin of the El Dragón Selenium Mineralization, Quijarro Province, Potosí, Bolivia. *Minerals* **2017**, *7*, 68. [[CrossRef](#)]
52. Wall, F.J. *Statistical Data Analysis Handbook*; McGraw-Hill Inc.: New York, NY, USA, 1986; 546p.
53. Konnert, J.A.; Evans, H.T., Jr.; McGee, J.J.; Ericksen, G.E. Mineralogical studies of the nitrate deposits of Chile: VII. Two new saline minerals with the composition $\text{K}_6(\text{Na,K})_4\text{Na}_6\text{Mg}_{10}(\text{XO}_4)_{12}(\text{IO}_3)_{12}\cdot 12\text{H}_2\text{O}$: Fuenzalidaite ($\text{X} = \text{S}$) and carlosruizite ($\text{X} = \text{Se}$). *Am. Mineral.* **1994**, *79*, 1003–1008.
54. Shuvalov, R.R.; Vegasova, L.P.; Semenova, T.F.; Filatov, S.K.; Krivovichev, S.V.; Siidra, O.I.; Rudashevsky, N.S. Prewittite, $\text{KPb}_{1.5}\text{Cu}_6\text{Zn}(\text{SeO}_3)_2\text{O}_2\text{Cl}_{10}$, a new mineral from Tolbachik fumaroles, Kamchatka peninsula, Russia: Description and crystal structure. *Am. Miner.* **2013**, *98*, 463–469. [[CrossRef](#)]
55. Cesbron, F.; Oosterbosch, R.; Pierrot, R. Une nouvelle espèce minérale: La marthozite. Uranyl-sélénite de cuivre hydraté. *Bull. Soc. Fr. Minéral. Cristallogr.* **1969**, *92*, 278–283. [[CrossRef](#)]
56. Cooper, M.A.; Hawthorne, F.C. Structure topology and hydrogen bonding in marthozite, $\text{Cu}^{2+}[(\text{UO}_2)_3(\text{SeO}_3)_2\text{O}_2](\text{H}_2\text{O})_8$, a comparison with guilleminite, $\text{Ba}[(\text{UO}_2)_3(\text{SeO}_3)_2\text{O}_2](\text{H}_2\text{O})_3$. *Can. Mineral.* **2001**, *39*, 797–807. [[CrossRef](#)]
57. Lussier, A.J.; Lopez, R.A.K.; Burns, P.C. A revised and expanded structure hierarchy of natural and synthetic hexavalent uranium compounds. *Can. Mineral.* **2016**, *54*, 177–283. [[CrossRef](#)]

58. Krivovichev, S.V.; Burns, P.C. Geometrical isomerism in uranyl chromates I. Crystal structures of $(\text{UO}_2)(\text{CrO}_4)(\text{H}_2\text{O})_2$, $[(\text{UO}_2)(\text{CrO}_4)(\text{H}_2\text{O})_2](\text{H}_2\text{O})$ and $[(\text{UO}_2)(\text{CrO}_4)(\text{H}_2\text{O})_2]_4(\text{H}_2\text{O})_9$. *Z. Kristallogr.* **2001**, *218*, 568–574. [[CrossRef](#)]
59. Krivovichev, S.V.; Burns, P.C. Geometrical isomerism in uranyl chromates II. Crystal structures of $\text{Mg}_2[(\text{UO}_2)_3(\text{CrO}_4)_5](\text{H}_2\text{O})_{17}$ and $\text{Ca}_2[(\text{UO}_2)_3(\text{CrO}_4)_5](\text{H}_2\text{O})_{19}$. *Z. Kristallogr.* **2001**, *218*, 683–690. [[CrossRef](#)]
60. Krivovichev, S.V. *Structural Crystallography of Inorganic Oxysalts*; Oxford University Press: Oxford, UK, 2009; 324p.
61. Almond, P.M.; Albrecht-Schmitt, T.E. Hydrothermal synthesis and crystal chemistry of the new strontium uranyl selenites, $\text{Sr}[(\text{UO}_2)_3(\text{SeO}_3)_2\text{O}_2]\cdot 4\text{H}_2\text{O}$ and $\text{Sr}[(\text{UO}_2)(\text{SeO}_3)_2]\cdot 2\text{H}_2\text{O}$. *Am. Mineral.* **2004**, *89*, 976–980. [[CrossRef](#)]
62. Dunn, P.J.; Pecker, D.R.; Sturman, B.D. Mandarininite—New ferric-iron selenite from Bolivia. *Can. Mineral.* **1978**, *16*, 605–609.
63. Lasmanis, R.; Nagel, J.; Sturman, B.D.; Gait, R.I. Mandarininite from the De Lamar silver mine, Owyhee County, Idaho, U.S.A. *Can. Mineral.* **1981**, *19*, 409–410.
64. Camprostrini, I.; Gramaccioli, C.M. Selenium-rich secondary minerals from the Baccu Locci mine (Sardinia, Italy). *Neues Jahrb. Mineral. Abh.* **2001**, *177*, 37–59. [[CrossRef](#)]
65. Zhu, J.-M.; Johnson, T.M.; Finkelman, R.B.; Zheng, B.-S.; Sýkorová, I.; Pešek, J. The occurrence and origin of selenium minerals in Se-rich stone coals, spoils and their adjacent soils in Yutangba, China. *Chem. Geol.* **2012**, *330–331*, 27–38. [[CrossRef](#)]
66. Grundmann, G.; Förster, H.-J. The Sierra de Cacheuta vein-type Se mineralization, Mendoza Province, Argentina. *Minerals* **2018**, *8*, 127. [[CrossRef](#)]
67. Hawthorne, F.C. The crystal structure of mandarininite, $\text{Fe}^{3+}_2\text{Se}_3\text{O}_9\cdot 6\text{H}_2\text{O}$. *Can. Mineral.* **1984**, *22*, 475–480.
68. Holzheid, A.; Charykova, M.V.; Krivovichev, V.G.; Ledwig, B.; Fokina, E.L.; Poroshina, K.L.; Platonova, N.V.; Gurzhiy, V.V. Thermal behavior of ferric selenite hydrates ($\text{Fe}_2(\text{SeO}_3)_3\cdot 3\text{H}_2\text{O}$, $\text{Fe}_2(\text{SeO}_3)_3\cdot 5\text{H}_2\text{O}$) and the water content in the natural ferric selenite mandarininite. *Chem. Erde* **2018**, *78*, 228–240. [[CrossRef](#)]
69. Lelet, M.I.; Charykova, M.V.; Holzheid, A.; Ledwig, B.; Krivovichev, V.G.; Suleimanov, E.V. A calorimetric and thermodynamic Investigation of the synthetic analogue of mandarininite, $\text{Fe}_2(\text{SeO}_3)_3\cdot 5\text{H}_2\text{O}$. *Geosciences* **2018**, *8*, 391. [[CrossRef](#)]
70. Back, M.E.; Grice, J.D.; Gault, R.A.; Cooper, M.A.; Walford, P.C.; Mandarino, J.A. Telluromandarininite, a new tellurite mineral from the El Indio-Tambo, Mining Property, Andes Mountains, Chile. *Can. Mineral.* **2017**, *55*, 21–28. [[CrossRef](#)]
71. Krivovichev, S.V. Combinatorial topology of salts of inorganic oxoacids: Zero-, one- and two-dimensional units with corner-sharing between coordination polyhedra. *Crystallogr. Rev.* **2004**, *10*, 185–232. [[CrossRef](#)]
72. Krivovichev, S.V. Topology of microporous structures. *Rev. Mineral. Geochem.* **2005**, *57*, 17–68. [[CrossRef](#)]
73. Krivovichev, S.V. Structure description, interpretation and classification in mineralogical crystallography. *Crystallogr. Rev.* **2017**, *23*, 2–71. [[CrossRef](#)]
74. Krivovichev, S.V.; Mentré, O.; Siidra, O.I.; Colmont, M.; Filatov, S.K. Anion-centered tetrahedra in inorganic compounds. *Chem. Rev.* **2013**, *113*, 6459–6535. [[CrossRef](#)] [[PubMed](#)]
75. Krivovichev, S.V.; Starova, G.L.; Filatov, S.K. “Face-to-face” relationships between oxocentered tetrahedra and cation-centered tetrahedral oxyanions in crystal structures of minerals and inorganic compounds. *Mineral. Mag.* **1999**, *63*, 263–266. [[CrossRef](#)]
76. Vergasova, L.P.; Semenova, T.F.; Filatov, S.K.; Krivovichev, S.V.; Shuvalov, R.R.; Ananiev, V.V. Georgbokiite $\text{Cu}_5\text{O}_2(\text{SeO}_3)_2\text{Cl}_2$ —A new mineral from volcanic sublimates. *Dokl. Akad. Nauk* **1999**, *364*, 527–531. (In Russian)
77. Vergasova, L.P.; Krivovichev, S.V.; Filatov, S.K.; Britvin, S.N.; Burns, P.C.; Ananyev, V.V. Parageorgbokiite, $\beta\text{-Cu}_5\text{O}_2(\text{SeO}_3)_2\text{Cl}_2$ —A new mineral from volcanic exhalations (Kamchatka peninsula, Russia). *Zap. Ross. Mineral. Obshch.* **2006**, *135*, 24–28. (In Russian) [[CrossRef](#)]
78. Vergasova, L.; Krivovichev, S.; Semenova, T.; Filatov, S.; Ananiev, V. Chloromenite, $\text{Cu}_9\text{O}_2(\text{SeO}_3)_4\text{Cl}_6$, a new mineral from the Tolbachik volcano, Kamchatka, Russia. *Eur. J. Mineral.* **1999**, *11*, 119–123. [[CrossRef](#)]
79. Krivovichev, S.V.; Gorelova, L.A. Se–Cl interactions in selenite chlorides: A theoretical study. *Crystals* **2018**, *8*, 193. [[CrossRef](#)]

80. Vergasova, L.P.; Semenova, T.F.; Krivovichev, S.V.; Filatov, S.K.; Zolotarev, A.A., Jr.; Ananiev, V.V. Nicksobolevite, $\text{Cu}_7(\text{SeO}_3)_2\text{O}_2\text{Cl}_6$, a new complex copper oxoselenite chloride from Tolbachik fumaroles, Kamchatka peninsula, Russia. *Eur. J. Mineral.* **2014**, *26*, 439–449. [[CrossRef](#)]
81. Kovrugin, V.M.; Korniyakov, I.V.; Gurzhiy, V.V.; Siidra, O.I.; Colmont, M.; Mentre, O.; Krivovichev, S.V. Synthesis and crystal structure of $\beta\text{-CuSe}_2\text{O}_5$, a new polymorph of copper diselenite. *Mendeleev Commun.* **2017**, *27*, 61–63. [[CrossRef](#)]
82. Olds, T.A.; Plášil, J.; Kampf, A.R.; Simonetti, A.; Sadergaski, L.R.; Chen, Y.S.; Burns, P.C. Ewingite: Earth's most complex mineral. *Geology* **2017**, *45*, 1007–1010. [[CrossRef](#)]



© 2019 by the authors. Licensee MDPI, Basel, Switzerland. This article is an open access article distributed under the terms and conditions of the Creative Commons Attribution (CC BY) license (<http://creativecommons.org/licenses/by/4.0/>).